Mapping the Internal Geometry of Tactile Space

Matthew R. Longo and Olga Golubova

Department of Psychological Sciences, Birkbeck, University of London

Address correspondence to:

Matthew R. Longo

Department of Psychological Sciences

Birkbeck, University of London

Malet Street

London WC1E 7HX

United Kingdom

m.longo@bbk.ac.uk

Abstract

A large body of research has shown spatial distortions in the perception of tactile distances on the skin. For example, perceived tactile distance is increased on sensitive compared to less sensitive skin regions, and larger for stimuli oriented along the medio-lateral axis than the proximo-distal axis of the limbs. In this study we aimed to investigate the spatial coherence of these distortions by reconstructing the internal geometry of tactile space using multidimensional scaling (MDS). Participants made verbal estimates of the perceived distance between two touches applied sequentially to locations on their left hand. In Experiment 1 we constructed perceptual maps of the dorsum of the left hand, which showed a good fit to the actual configuration of stimulus locations. Critically, these maps also showed clear evidence of spatial distortion, being stretched along the medio-lateral hand axis. Experiment 2 replicated this result and showed that no such distortion is apparent on the palmar surface of the hand. These results show that distortions in perceived tactile distance can be characterized by geometrically simple and coherent deformations of tactile space. We suggest that the internal geometry of tactile space is shaped by the geometry of receptive fields in somatosensory cortex.

Statement of Public Significance

The perceived distance between touches on the skin is known to differ across body parts and between orientations within a single part. This study develops a novel method of measuring perceptual maps of touch to clarify the nature of these distortions.

Several forms of perception require that immediate sensory signals be combined with information about the size and shape of the body. For example, using the temporal difference in the arrival time of sound at the two ears to localize an auditory stimulus requires information about the distance between the ears (Clifton et al., 1988). Similarly, the use of convergence angles for absolute judgments of visual distance requires information about inter-ocular distance (Banks, 1988). In the classic study of Warren and Whang (1987), the authors showed that the perceived height of the eyes off the ground also structures perception. By inserting (unbeknownst to participants) a false floor between the participants and an aperture, and thus reducing effective eye-height, they showed that the perception of the affordance of passability through the aperture was determined as a fixed proportion of perceived eye-height.

Warren and Whang (1987) introduced a distinction between two ways in which visual information specifying affordances of the environment might be coded, *extrinsically* or *intrinsically*. In the case of extrinsic coding, visual information is first used to specify the dimensions of environmental stimuli in an absolute, viewer-independent metric, which is then subsequently compared to representations of the size of the viewer's body. In intrinsic coding, in contrast, visual information is related directly to physical dimensions of the observer in body-scaled units. By showing that visual information for judgments of the possibility of apertures appears to be directly scaled in terms of eyeheight, Warren and Whang provided evidence in favour of the role of intrinsic coding for the visual perception of affordances. This distinction between intrinsic and extrinsic coding is particularly intriguing in the sense of touch. Given that the primary receptor surface (the skin) is physically co-extensive with the body itself, tactile information is fundamentally intrinsic in a way that visual information need not

be. Touch, however, can clearly also be used to perceive the extrinsic physical

properties of objects.

Distortions of Tactile Distance Perception

Longo, Azañón, and Haggard (2010) argued that perceiving the metric properties

of objects touching the skin requires that immediate sensory signals be combined with

stored representations of body size and shape, what they called a *body model*. Indeed,

several recent studies have shown relations between the perceived size of the body and

perceived tactile distance on the skin. For example, perceived tactile distance or size has

been found to be modulated by alterations of perceived body size induced through

manipulations such as visual magnification (Taylor-Clarke, Jacobsen, & Haggard, 2004),

proprioceptive self-touch illusions (de Vignemont, Ehrsson, & Haggard, 2005),

cutaneous anesthesia (Berryman, Yau, & Hsiao, 2006), sounds produced by action

(Tajadura-Jiménez et al., 2012, 2015), the rubber hand illusion (Bruno & Bertamini,

2010), and tool use (Canzoneri et al., 2013; Miller, Longo, & Saygin, 2014, 2017). Thus,

in analogy with the modulation of perceived passability of apertures when apparent

eyeheight was altered shown by Warren and Whang (1987), these results show that

experimental manipulations of represented body size alter perceived tactile distance.

Perceived tactile distance is not, however, shaped only by high-level models of

the body, but also by low-level aspects of somatosensory organization. For example,

Weber (1834/1996) found that the perceived distance between two points of a

compass changed as he moved them across his skin, feeling farther apart on regions of

high tactile sensitivity compared to regions of lower sensitivity. Subsequent studies

have replicated this pattern and suggest a systematic relation between perceived tactile

distance and the spatial sensitivity of skin surfaces (e.g., Cholewiak, 1999; Taylor-Clarke

et al., 2004; Anema, Wolswijk, Ruis, & Dijkerman, 2008; Miller, Longo, & Saygin, 2016), an effect known as *Weber's illusion*, suggesting that tactile distance perception preserves spatial distortions characteristic of the famous 'Penfield homunculus' (Penfield & Boldrey, 1937).

While Weber's illusion shows distortions in the relative size of perceived tactile distance on different skin surfaces, similar illusions have also been shown within individual skin surfaces as a function of orientation. For example, Longo and Haggard (2011) asked participants to make forced-choice judgments about which of two tactile distances felt bigger, applying one in the medio-lateral axis of the hand dorsum (*across* the hand) and one in the proximo-distal axis (*along* the hand). There was a large bias to perceived distances oriented along the medio-lateral axis as larger. Similar results have also been found on the forearm (Green, 1982; Le Cornu Knight, Longo, & Bremner, 2014), the leg (Green, 1982), and the face (Longo, Ghosh, & Yahya, 2015). Such anisotropies are in line with the overall pattern of Weber's illusion given that tactile acuity is known to be higher in the medio-lateral than in the proximo-distal axis of the limbs (Weber, 1834/1996; Cody, Gaarside, Lloyd, & Poliakoff, 2008). Moreover, they also mirror anisotropies in the shape of tactile receptive fields (RFs) in somatosensory cortex, which tend to be oval-shaped, rather than circular, with the long axis oriented along the proximo-distal limb axis (e.g., Powell & Mountcastle, 1959; Brooks, Rudomin, & Slayman, 1961; Alloway, Rosenthal, & Burton, 1989). Intriguingly, the magnitude of this perceptual anisotropy is reduced or eliminated on the glabrous skin of the palm (Longo & Haggard, 2011; Le Cornu Knight et al., 2014; Longo, Ghosh, et al., 2015), a surface with more circular receptive fields than the dorsum (DiCarlo, Johnson, & Hsiao, 1998; DiCarlo & Johnson, 2002).

5

To account for this overall pattern of results, we proposed a 'pixel' model of perceived tactile distance (Longo & Haggard, 2011; Longo, 2017). The key idea of this model is that tactile space consists of a two-dimensional array, with the RFs of neurons in a somatotopic map being treated as the pixels comprising this array. Judging distance would then involve counting the number of pixels separating two touched locations. Because RFs are smaller on sensitive skin surfaces than on less sensitive surfaces (Powell & Mountcastle, 1959; Sur, Merzenich, & Kaas, 1980), a given tactile distance will cover more pixels on a sensitive surface, consistent with Weber's illusion. Similarly, where RFs are oval-shaped, tactile distances oriented along the shorter axis of the ovals will cover more pixels than those oriented along the longer axis, consistent with the anisotropies described in the previous paragraph.

A central prediction of the pixel model is that distortions of tactile distance perception should be geometrically coherent. Where RFs differ in size, the model predicts a relative magnification of the skin surface with smaller RFs. Where RFs are oval-shaped, the model predicts stretch along the short axis of the ovals. In either case, the pixel model predicts that the distortion induced should reflect a geometrically simple stretch of tactile space. A century ago, D'Arcy Thompson (1917) argued that many differences in biological form, whether between species or as a function of developmental change, could be characterized by geometrically simple *transformations*. Thompson asked how one form would need to be deformed, or stretched, to transform it into another, finding that even visually-dramatic differences could be achieved through geometrically-simple transformations, such as stretches and skews. The pixel model, similarly, predicts that tactile space, while distorted, should nevertheless be related to the true structure of the skin in a geometrically straightforward way. While previous studies have revealed the existence of distortions of perceived tactile distance,

we aimed here to characterize these distortions in a more holistic manner than is possible with forced-choice comparisons. We thus constructed perceptual maps of the skin surface reflecting perceived distance between different locations and asked how these maps deform the true structure of the skin.

Mapping Representational Structure with Multidimensional Scaling

Several previous studies have attempted to construct perceptual maps of the body, for example by measuring patterns of proprioceptive localization of body parts (e.g., Longo & Haggard, 2010, 2012), localization of individual somatic stimuli in both skin-centred (e.g., Rapp, Hendel, & Medina, 2002; Mancini, Longo, Iannetti, & Haggard, 2011) and external (e.g., Trojan et al., 2006; Longo, Mancini, & Haggard, 2015) frames of reference, and localization of body parts relative to an anchor part (e.g., Fuentes, Longo & Haggard, 2013; Fuentes, Pazzaglia, Longo, Scivoletto, & Haggard, 2013). In each of these cases, perceptual maps were constructed directly, in the sense that participants were asked to make overt judgments of perceived location in some external frame of reference. Thus, the tasks were extrinsic in the sense of Warren and Whang (1987). Here, we adopted a different, and more indirect approach, asking only for judgments of perceived *distance* between pairs of touches, rather than the perceived location of individual landmarks. We then reconstructed perceptual maps from the pattern of distance judgments using multidimensional scaling (MDS). MDS is a method for reconstructing the latent spatial structure underlying a set of items given a matrix of pairwise distances or dissimilarities between items (Shepard, 1980; Everitt & Rabe-Hesketh, 1997; Cox & Cox, 2001). As with principal components analysis, it is frequently possible to preserve a large proportion of the variance in the data using a small number

of dimensions. We aimed to use MDS to reconstruct the internal geometry of tactile space.

Consider the standard textbook example of MDS, which involves the distances between each pair of a set of cities, usually in the author's home country. For example, we might start with the shortest driving distance between each pair of ten American cities (e.g., New York to Boston, Boston to Los Angeles, Los Angeles to Chicago, etc.). The resulting 10x10 distance matrix is symmetrical (i.e., the distance from San Diego to Chicago is the same as from Chicago to San Diego) and with zeros on the diagonal (i.e., the distance from Philadelphia to Philadelphia is 0 km). MDS applied to this distance matrix yields coordinates for each of the ten cities in a space of up to ten dimensions such that the distances between the cities in the high-dimensional space are as proportional as possible to the actual distances. Given that the data reflect distances between cities, we clearly expect that the best two dimensions should account for a very large percentage of the total variance in the data. A two-dimensional solution will not perfectly reconstruct the distances, given factors such as measurement error, curvature of the Earth, differences in elevation of the cities, and idiosyncrasies of the road network. Nevertheless, the first two dimensions of the MDS solution will produce a configuration very similar to a map of the United States (though the configuration produced may need to be reflected and rotated to match our familiar map).

Within psychology, the use of MDS has been related to the idea that the judged similarity between two concepts, or the extent to which learning will generalize between them, is related to their proximity in some 'psychological space' (Shepard, 1987; Gärdenfors, 2000). Given data on the similarity or confusability of stimuli or concepts, MDS can be used to reconstruct the geometric structure of the underlying psychological space. This method has been widely used to explore the psychological

spaces underlying domains such as colour (e.g., Shepard & Cooper, 1992; Bosten,

Robinson, Jordan, & Mollon, 2005), visual space perception (Aznar-Casanova,

Matsushima, Ribeiro-Filho, & Da Silva, 2006), facial appearance (e.g., Byatt & Rhodes,

2004; Rhodes, 2013), object categorization (e.g., Nosofsky, 1986), visual shape

perception (e.g., Cutzu & Edelman, 1996), emotion (e.g., Feldman Barrett & Fossum,

2001; Kring, Feldman Barrett, & Gard, 2003), mathematics (e.g., Griffiths & Kalish,

2002), odors (e.g., Carrie, Scannell, & Dawes, 1999), music (e.g., Krumhansl & Kessler,

1982; Shepard, 1982; Kendall & Carterette, 1991), tactile texture perception (e.g.,

Hollins, Bensmaïa, Karlof, & Young, 2000), pain (e.g., Clark, Carroll, Yang, & Janal, 1986;

Clark, Ferrer-Brechner, Janal, Carroll, & Yang, 1989), perception of risks (e.g., Johnson &

Tversky, 1984), verb semantics (e.g., Wolff & Song, 2003), and even the perception of

letters in pigeons (Blough, 1982). MDS has been used similarly in neuroscience, for

example to reveal representational structure in the ventral visual pathway (e.g., Young

& Yamane, 1992; Kriegeskorte et al., 2008), categorical representations of speech in

auditory cortex (e.g., Chang et al., 2010), and global patterns of functional brain

connectivity (e.g., Friston, Frith, Fletcher, Liddle, & Frackowiak, 1996).

The Present Study

    Here we used MDS to reconstruct the internal geometry of tactile space. We

asked participants to judge the perceived distance between pairs of touches and applied

MDS to the resulting matrix of perceived distances to construct perceptual maps of the

representation of the skin. The logic is exactly analogous to the textbook example of

MDS described above to reconstruct a map of the United States from a matrix of driving

distances between pairs of American cities. The only difference is that we use a matrix

of *perceived*, rather than actual distances. The advantage of this method is that it

produces an overall map of the geometry of tactile space, allowing us to investigate the way in which tactile space deforms the true spatial layout of the skin. In Experiment 1 participants made verbal judgments of the perceived distance between touches applied to each pair of a 4x4 grid on the dorsum of their left hand. We show that two-dimensional perceptual maps can be constructed which show good fit to the actual shape of the skin, but are also clearly distorted, showing stretch along the medio-lateral hand axis in comparison to the proximo-distal axis. Experiment 2 replicated this finding and extended it to the palm of the hand, showing that while similarly clear perceptual maps can be constructed on both surfaces, distortion is apparent only on the dorsal and not on the palmar hand surface.

Experiment 1

Methods

Participants

Twelve members of the Birkbeck community (six female) between 18 and 51 years of age (*M*: 28.0 years; *SD*: 9.1) participated for payment or course credit. All were right-handed as assessed by the Edinburgh Inventory (Oldfield, 1971). Participants were naïve to the experimental hypotheses and provided written informed consent. Procedures were approved by the local ethics committee and were in line with the principles of the Declaration of Helsinki.

Procedure

To identify stimulus locations, a 4x4 grid of points was marked with a pen on the back of the participant's left hand using a plastic template (see Figure 1). Adjacent points on the grid were separated by 1.5 cm. The four rows of points ran along the

medio-lateral hand axis, while the four columns ran along the proximo-distal axis. The

proximo-distal axis was operationalized by the tendon connecting the *extensor*

digitorum muscle to the middle finger. Tactile stimulations were applied using a von

Frey hair (1765 milliNewtons). The use of a von Frey hair ensures that the amount of

pressure applied at each location was constant across stimulations.

Figure 1: Example of the 4x4 grid of stimulation locations.

During testing, the participant sat at a table with their left hand lying palm-down.

The experimenter sat at the table across from the participant to apply tactile stimuli.

The participant was blindfolded throughout the experiment and was not allowed to see

the grid drawn on their hand until after the experiment. On each trial, two locations

were stimulated in sequence by the experimenter. Each location was stimulated for

approximately one second with a one second inter-stimulus interval. After each trial, participants made unspeeded verbal estimates of the perceived distance between two stimulus locations by giving a number in millimeters. Participants were instructed to be as precise as possible in their estimates, but also to not spend a lot of time thinking about responses and to report whichever distance felt immediately intuitive. Participants were allowed to give a response of 0 mm if they felt like the same location had been stimulated twice, though in fact two different locations were stimulated on each trial.

There are 120 possible pairs of 16 stimulus locations and two stimulus orders for each pair, making 240 types of trials. Each trial type was presented twice, resulting in 480 trials. These were divided into four blocks of 120 trials separated by short breaks. The trials were presented in random sequence subject to the restriction that each of the 240 trial types occurred exactly once in blocks 1-2 and once in blocks 3-4.

At the end of the experiment, a photograph was taken of each participant's hand showing the locations of the landmarks. Pixel coordinates of each landmark were coded offline. A ruler appeared next to the hand in each photograph, allowing conversion between distances in pixels and cm.

Multidimensional Scaling

The four repetitions of each stimulus pair for an individual participant were averaged (collapsing across order of stimulation), resulting in a symmetric matrix reflecting the pairwise perceived distance between pairs of points, with zeros on the diagonal. Classical multidimensional scaling was applied to the distance matrix for each participant using the cmdscale command in MATLAB (Mathworks, Natick, MA). The

output of MDS is a set of eigenvalues for each dimension and coordinates for each landmark in each dimension.

As there are 16 landmarks, MDS attempts to position the landmarks in 16-dimensional space such that the distances between them are as proportional as possible to the perceived distances. In most real datasets, however, it will not be possible to find a configuration which perfectly preserves these distances. This is due to violations of the triangle inequality, which states that the distance between landmarks A and C cannot be greater than the sum of the distances between landmarks A and B and between B and C. As an example, if the distance between London and Oxford is 100 miles, and the distance between Oxford and Manchester is 200 miles, then the distance from London to Manchester cannot be greater than 300 miles, since we know at least one route (via Oxford) of that distance. It is, of course, perfectly possible for participants to produce patterns of perceptual judgments which violate this inequality (mathematically, this implies that the distance matrix is not positive semi-definite), in which case the MDS solution will not perfectly reconstruct the perceived distances. In this case, MDS will produce a configuration with a dimensionality less than 16, the missing dimensions being associated with negative eigenvalues. Therefore, to calculate the percentage of variance in the data accounted for by each dimension, we compared the absolute value of each eigenvalue to the sum of the absolute values of all 16 eigenvalues.

In order to create a null distribution for comparison with our data, we conducted MDS on simulated random data. For each simulation, 120 random numbers were generated and placed into a distance matrix, as with the actual data. MDS was applied to each simulation and the eigenvalues and coordinates extracted. One million such simulations were conducted.

Procrustes Alignment

Procrustes alignment (Rholf & Slice, 1990; Goodall, 1991) superimposes two spatial configurations of homologous landmarks by translating, scaling, and rotating them to be as closely aligned as possible. First, the two configurations are translated so that their centroids (i.e., the centre of mass of all landmarks) are in the same location. Second, the configurations are normalized in size so that the centroid size, the square root of the sum of squared distances between each landmark and the centroid, is equal to 1. Third, the configurations are rotated to minimize the sum of squared distance between pairs of homologous landmarks. Note that in the present study mirror reflections of the configurations were allowed, though in other contexts this may not be desirable. At this point, the configurations are in the best possible spatial alignment, with all non-shape differences removed (Bookstein, 1991).

We used Procrustes alignment in two ways, both as a way to quantify dissimilarity in shape and as a visualization tool. First, the residual sum of squared distances between pairs of homologous landmarks which is not removed by Procrustes alignment provides a measure of the dissimilarity in shape between the two configurations, called the *Procrustes Distance*. If two configurations have exactly the same shape, they will lie on top of each other following Procrustes alignment and thus have a Procrustes distance of 0. In contrast, two configurations with no shared spatial structure at all will have a Procrustes distance of 1, given that the size normalization results in a total sum of squared variance within each configuration of exactly 1. Second, Procrustes alignment provides a natural way to visually display configurations, making differences in shape clearly apparent.

Results and Discussion

The left panel of Figure 2 shows a scree plot depicting the mean percentage of variance in the data explained by each dimension in participants' judgments (in blue) and in one million simulations of random data (green). As described above, the lines are not monotonically decreasing (as in familiar scree plots from principal component analysis) because violations of the triangle inequality result in non-real variance, and thus negative eigenvalues. There was clear support for a two-dimensional solution in terms of the traditional scree test, as there is a clear drop-off in the amount of variance explained after the second dimension, but only modest drop-offs thereafter. A two-dimensional solution was also strongly supported by comparing the actual data to the simulations, since the first two dimensions were the only ones in which the amount of variance explained in the data exceeded that in the stimulated random data. The first two dimensions accounted on average for 28.7% and 17.7% of the variance in the data, for a sum of 46.4%. By comparison, none of the simulations had a first dimension explaining as much as the average of our data (i.e., $p < 0.000001$), while only 10 simulations had a second dimension explaining as much as the average of our data (i.e., $p = 0.00001$).
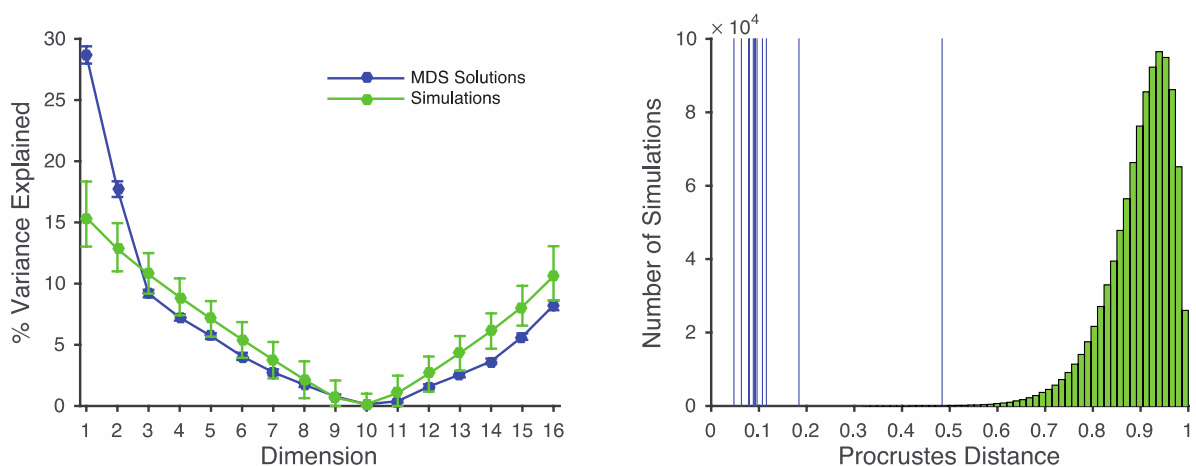

Figure 2: *Left panel*: Scree plot showing the mean percentage variance explained by each of the 16 MDS dimensions for perceived distance judgments in Experiment 1 (blue) and for one million simulations of random distance matrices (green). The blue error bars indicate one standard error

of the mean for perceptual judgments. The green error bars, in contrast, show the range of the center 95% of values from individual simulations (note that this is a much wider interval than the usual 95% confidence interval which concerns the location of the mean, rather than individual values). The results provided strong support for a two-dimensional solution, both by the traditional scree test and as the amount of variance explained in the perceptual data exceeded that for the simulations only in the first two dimensions. *Right panel*: Histogram showing the distribution of Procrustes distances between two-dimensional MDS solutions from simulations and a perfectly square 4x4 grid. Blue vertical lines indicate the corresponding Procrustes distance for the perceptual judgments of each participant. These values were much smaller than the simulations, showing that perceptual maps mirror the actual spatial layout of the skin.

The preceding analysis shows the participants' perceptual maps are two-dimensional, mirroring the dimensionality of the stimulated skin region itself. This, however, does not imply that these maps accurately reflect the true spatial organization of the skin. To investigate this, we calculated the dissimilarity in shape (i.e., the Procrustes distance) between a perfectly square 4x4 grid and the first two dimensions from each MDS configuration. These results are shown in the right panel of Figure 2. The green bars show a histogram of the Procrustes distances of the simulations with the square grid, while the vertical blue lines reflect the Procrustes distance for each participant's perceptual map. Eleven participants had a smaller Procrustes distance than any of the simulations. Only one fell within the range of the simulations, having a value larger than 134 of one million simulations (i.e., $p = 0.000134$). These results clearly demonstrate that the perceptual maps of tactile space preserve the true spatial structure of the skin. The maps themselves are shown in Figure 3.
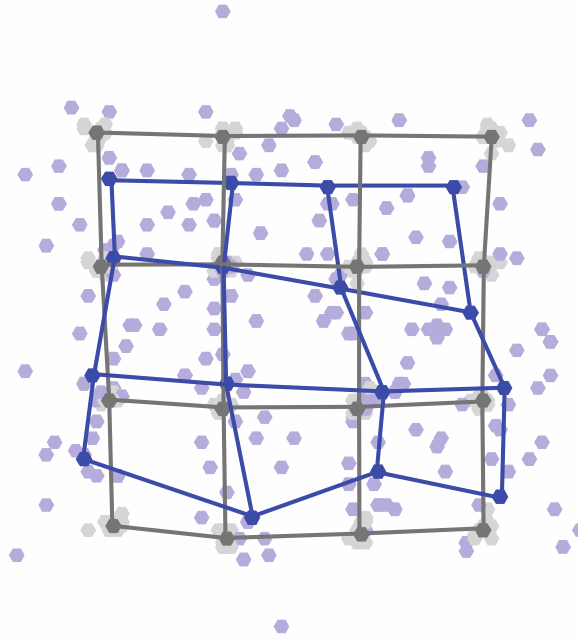
Figure 3: Perceptual maps of the hand dorsum in Experiment 1. Pale blue dots are landmarks from individual participants' maps, each put into Procrustes alignment with an ideal square grid. The pale grey dots are the same but for the actual locations of the landmarks on participants' hands. The dark dots and lines reflect the grand average shape for perceptual maps (blue) and the actual configuration of landmarks (grey).

To assess distortions in the perceptual maps, we calculated the distance between pairs of landmarks that differed in location in either the medio-lateral axis (i.e., on the same row of landmarks) or the proximo-distal axis (i.e., on the same column of landmarks). Three types of distance were calculated: *small* distances, between adjacent stimulus locations; *medium* distances, between locations separated by one location; and *large* distances, separated by two locations (see left panel of Figure 4). There were 12 small, 8 mid, and 4 large distances in each orientation, which were averaged to yield one value for each combination of distance type and orientation for each participant. Distances in the medio-lateral orientation were farther apart than in the proximo-distal orientation for small (*M*: 0.191 vs. 0.161 Procrustes normalized units), $t(11) = 9.37$, $p < 0.0001$, $d_z = 2.71$, medium (*M*: 0.344 vs. 0.284 Procrustes normalized units), $t(11) = 4.39$, $p < 0.002$, $d_z = 1.27$, and large (*M*: 0.504 vs. 0.401 Procrustes normalized units), $t(11) = 4.06$, $p < 0.002$, $d_z = 1.17$, distances. We obtained an overall measure,

aggregating across the three sizes, by calculating the average distance per step, treating

small distances as one step, medium distances as two steps, and large distances as three

steps. With this aggregate measure there was a clear overestimation of distances in the

medio-lateral orientation (*M*: 0.173 vs. 0.141 Procrustes normalized units per step),
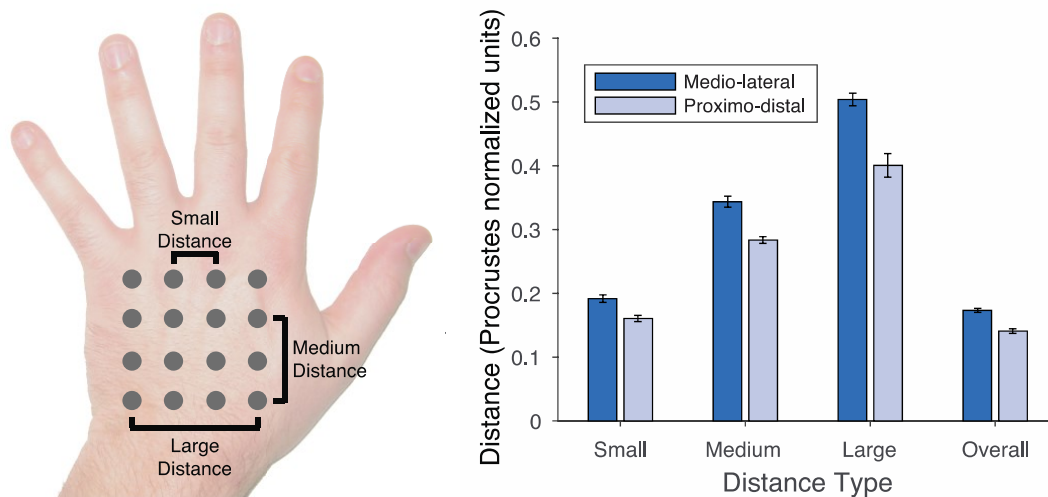
$t(11) = 4.86$, $p < 0.001$, $d_z = 1.40$.

Figure 4: *Left panel*: Examples of pairs of landmarks forming small, medium, and large distances. The small and large distances are in the medio-lateral orientation, while the medium distance is in the proximo-distal orientation. Within each orientation there were 12 small, 8 mid, and 4 large distances, which were averaged. *Right panel*: Mean distance in Procrustes normalized space between pairs of landmarks of each distance in the medio-lateral and proximo-distal orientations. There was clear overestimation of distances in the medio-lateral orientation, compared to the proximo-distal orientation. Error bars are one standard error of the mean.

Because the preceding analysis focuses entirely on pairs of landmarks exactly

aligned with either the medio-lateral or proximo-distal axis, we aimed to assess spatial

distortion also in a more holistic manner. We therefore adapted a procedure we

recently applied to quantifying distortions in position sense (Longo & Morcom, 2016).

Accordingly, we stretched a square grid reflecting the locations of the 16 points by

different amounts to find the stretch that minimized the Procrustes distance with each

participant's perceptual map, as well as with the actual configuration of points on their

hand. Stretches were defined by the multiplication of the x-coordinate (reflecting

location in the medio-lateral hand axis) by a stretch parameter. Thus, a stretch of 1 indicated a perfectly square grid, stretch of less than 1 indicated a tall thin grid, and stretch of more than 1 indicated a squat fat grid. Note that because Procrustes alignment normalizes size, a stretch applied to the medio-lateral axis is identical to the inverse stretch being applied to the proximo-distal axis (i.e., multiplying the x-coordinates by 2 is identical to multiplying the y-coordinates by 0.5). Thus, while distortions are described in terms of the medio-lateral axis, this method cannot indicate which specific axis is affected by distortions in the sense that stretch of one axis is formally identical to compression of the other. Values between 0.33 and 3 were tested by exhaustive search with a resolution of 0.0005 units in natural logarithm space (i.e., 4,415 steps). Note that we report mean stretch values as ratios, the statistical tests we report compare the mean logarithm of the ratios to 0, since ratios are not symmetrical around 1.

Figure 5 shows Procrustes distance as a function of stretch for both perceptual and actual hand maps. For the perceptual maps, the mean best-fitting stretch parameter was 1.252, significantly greater both than 1, $t(11) = 4.23$, $p < 0.002$, $d = 1.22$, and than parameters for the actual map, $t(11) = 5.19$, $p < 0.001$, $d_z = 1.50$. In contrast, for the actual configuration of points, the mean best-fitting stretch parameter was 0.957, significantly less than 1, $t(11) = -3.47$, $p < 0.01$, $d = 1.00$. This stretch in the proximo-distal axis is presumably due to the curvature of the hand being greater in the medio-lateral than the proximo-distal hand axis. This would have the result that distances between points in the medio-lateral orientation would be slightly smaller than distances in the proximo-distal orientation both in three-dimensional Euclidean space and in the two-dimensional projection onto the picture plane of the camera. Critically, to the extent that participants are sensitive to distance in 3-D space as opposed to distance

along the skin surface, this would work against our finding a bias for stretch in the medio-lateral axis.
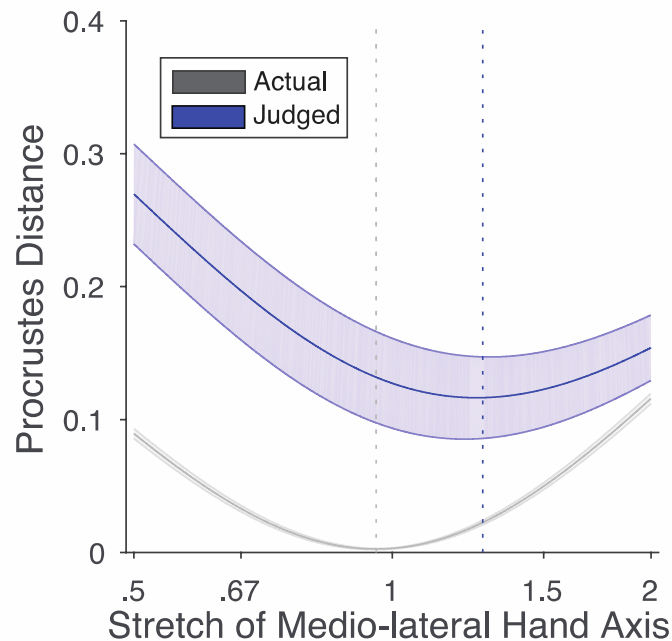

Figure 5: Mean Procrustes distance between actual (grey) and perceptual (blue) maps and idealized grids stretched by different amounts. A stretch of 1 indicates a square grid; stretches greater than 1 indicate stretch in the medio-lateral axis, while stretches less than 1 indicate stretch in the proximo-distal axis. The shaded regions indicate one standard error of the mean. The dotted vertical lines indicate the mean of the best-fitting stretches for perceptual maps (blue) and actual maps (grey). The stretch that minimized the Procrustes distance was substantially larger than 1. Thus, there was clear evidence for stretch in the medio-lateral hand axis for perceptual maps.

These results show that MDS can be used to construct perceptual maps of tactile space which show clear isomorphism with the actual configuration of the skin. These maps, however, also showed clear evidence of distortion, being stretched along the medio-lateral axis of the hand. This pattern of distortion is consistent with previous results that have directly compared the perceived distance between pairs of touches aligned with the proximo-distal and medio-lateral axes (e.g., Green, 1982; Longo & Haggard, 2011; Longo & Sadibolova, 2013). The current results show that this anisotropy can be characterized in terms of a geometrically coherent stretch of tactile space. On the pixel model (Longo & Haggard, 2011; Longo, 2017), this distortion is

20

related to the oval shape of somatosensory RFs on the hand dorsum (e.g., Alloway et al., 1989), which results in a pixel map which is stretched along the short axis of the RFs (i.e., the medio-lateral axis). Given that perceptual anisotropy in tactile distance perception is reduced or eliminated on the palm of the hand (e.g., Longo & Haggard, 2011; Le Cornu Knight et al., 2014; Longo, Ghosh, et al., 2015) and that somatosensory RFs on the palm are more circular than on the dorsum (e.g., Di Carlo & Johnson, 2002), Experiment 2 aimed to replicate the results from the first experiment and to extend them to the palm.

Experiment 2

Methods

Participants

Twenty-four members of the Birkbeck community (17 women) between 19 and 54 years of age (*M*: 32.5 years; *SD*: 7.9) participated for payment or course credit. All but four were right-handed as assessed by the Edinburgh Inventory. Two of the participants were excluded from analyses due to experimenter error, resulting in some stimulus pairs being duplicated and others not being presented at all.

Procedure

The procedures were similar to Experiment 1, except that stimuli were applied either to the dorsum of the left hand (as in Experiment 1) or to the palm, in separate blocks. There were two blocks of trials on each surface, with ABBA counterbalancing, and with the first condition counterbalanced across participants. As in Experiment 1 there were 120 trials per block. For each surface, there was one trial of each of the 240 combinations of stimulus locations and stimulation order.

Results and Discussion

The left column of Figure 6 shows scree plots depicting the mean percentage of variance in the data explained by each dimension for the dorsum (top left, in blue) and palm (bottom left, in red), as well as for the simulations (in green). As in Experiment 1, there was clear support for two-dimensional solutions on both skin surfaces, both in terms of the traditional scree test and in that the first two dimensions were the only ones in which the percentage of variance explained exceeded that of the simulations. On the dorsum, the first two dimensions accounted for an average of 26.4% and 17.5% of the variance in the data, for an average total of 43.9%. On the palm, they accounted for an average of 25.7% and 19.6%, for an average total of 45.3%. None of the simulations had a first dimension explaining as much variance as the average of our data for either the dorsum or the palm ($p < 0.0000001$). For the second dimension, there were no simulations that explained as much variance as the average of our data on the palm ($p < 0.0000001$) and only 28 on the dorsum ($p = 0.000028$). There was no significant difference between the amount of variance explained by the first two dimensions on the palm and on the dorsum, $t(21) = 1.02$, *n.s.*
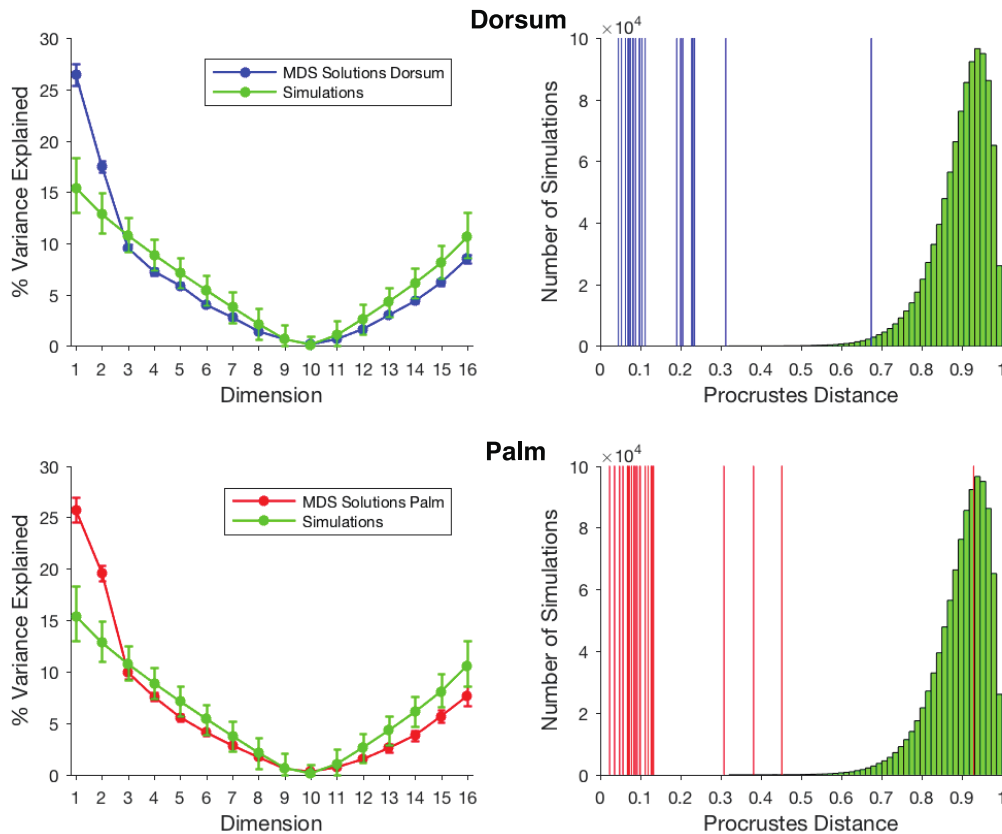
Figure 6: *Left panels*: Scree plots showing the mean percentage of variance explained by each of the 16 MDS dimensions for perceptual maps on the hand dorsum (top left, in blue) and palm (bottom left, in red) in Experiment 2. Results from one million simulations are shown in green in both panels. The blue and red error bars indicate one standard error of the mean. The green error bars show the range of the centre 95% of values from individual simulations. *Right panels*: Histograms showing the distribution of Procrustes distances between two-dimensional MDS solutions from simulations and a perfectly square 4x4 grid. The vertical lines show the corresponding values for individual participants for the dorsum (blue) and palm (red). These value were much smaller on average than the simulations, showing that perceptual maps mirror the actual spatial layout of the skin.

The right column of Figure 6 shows the dissimilarity in shape between perceptual maps from individual participants and a perfectly square grid assessed by the Procrustes distance. For the dorsum, only one of the participants had a perceptual map within the range of the simulations, having a value larger than 9,534 simulations (i.e., $p = 0.0095$). For the palm, three participants had perceptual maps within the range of the simulations. For two of these participants, their perceptual maps nevertheless showed reasonable similarity with the square grid, having Procrustes distances larger than 59 and 6 simulations, respectively (i.e., $p = 0.000059$ and 0.000006). One

participant, however, had a perceptual map with a Procrustes distance (0.929) very similar to the mean (0.898) and median (0.912) of the simulations. As there was no evidence that this map had any similarity at all with the true structure of the skin, this participant was removed from subsequent analyses. The maps themselves are shown in Figure 7. The mean Procrustes distance did not differ significantly between the dorsum and palm, $t(20) = 0.02$, *n.s.*
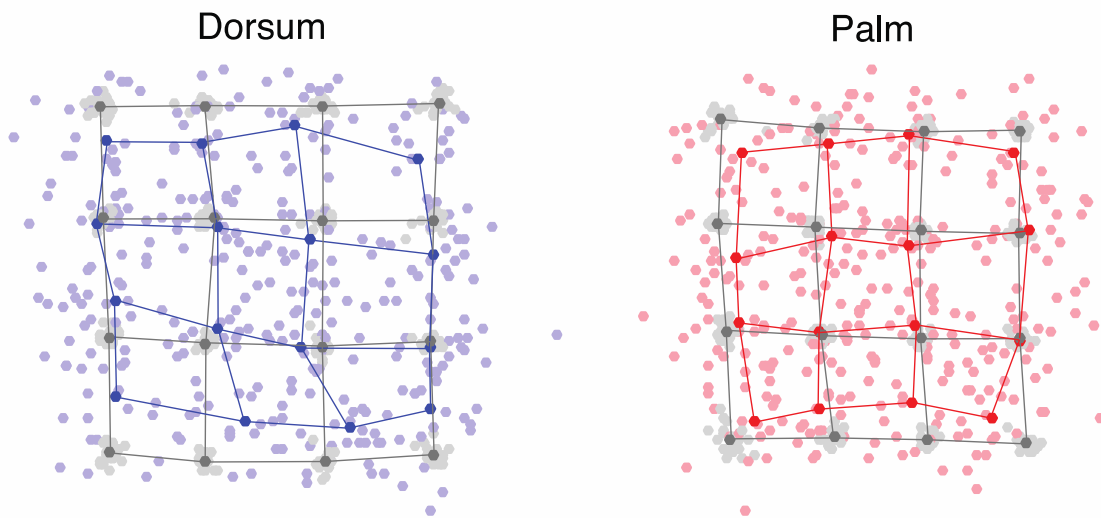

Figure 7: Perceptual maps of the hand dorsum (left panel, blue) and palm (right panel, red) in Experiment 2. Pale dots are landmarks from individual participants' perceptual maps (blue, red) or actual hand (grey), each put into Procrustes alignment with an ideal square grid. The dark dots represent the grand average shape for each type of map.

We assessed distortions in perceptual maps as in Experiment 1 by calculating the distance between pairs of landmarks differing in location in either the medio-lateral or proximo-distal axis. These data are shown in Figure 8. On the dorsum, distances in the medio-lateral orientation were farther apart than those in the proximo-distal orientation for small (*M*: 0.188 vs. 0.168 Procrustes normalized units), $t(20) = 3.26$, $p < 0.005$, $d_z = 0.71$, medium (*M*: 0.329 vs. 0.293 Procrustes normalized units), $t(20) = 2.88$, $p < 0.01$, $d_z = 0.63$, and large (*M*: 0.490 vs. 0.420 Procrustes normalized units), $t(20) = 4.31$, $p < 0.0005$, $d_z = 0.94$, distances, as well as in the aggregate measure (*M*: 0.168 vs. 0.147 Procrustes normalized units per step), $t(20) = 3.86$, $p < 0.001$, $d_z = 0.84$,

replicating the distortions reported in Experiment 1. In contrast, no such differences were found on the palm, whether for small (*M*: 0.177 vs. 0.179 Procrustes normalized units), $t(20) = -0.40$, *n.s.*, $d_z = 0.09$, medium (*M*: 0.313 vs. 0.310 Procrustes normalized units), $t(20) = 0.23$, *n.s.*, $d_z = 0.05$, or large (*M*: 0.456 vs. 0.452 Procrustes normalized units), $t(20) = 0.24$, *n.s.*, $d_z = 0.05$, distances, or overall (*M*: 0.158 vs. 0.157 Procrustes normalized units per step), $t(20) = 0.14$, *n.s.*, $d_z = 0.03$.

To compare distortions in the two orientations, we ran a 2x2 repeated-measures analysis of variance (ANOVA) on overall distance per step with skin surface (dorsum, palm) and orientation (medio-lateral, proximo-distal) as factors. There was a significant main effect of orientation, $F(1, 20) = 5.53$, $p < 0.03$, $\eta_p^2 = 0.217$, which was modulated by a significant interaction, $F(1, 20) = 12.61$, $p < 0.002$, $\eta_p^2 = 0.387$.
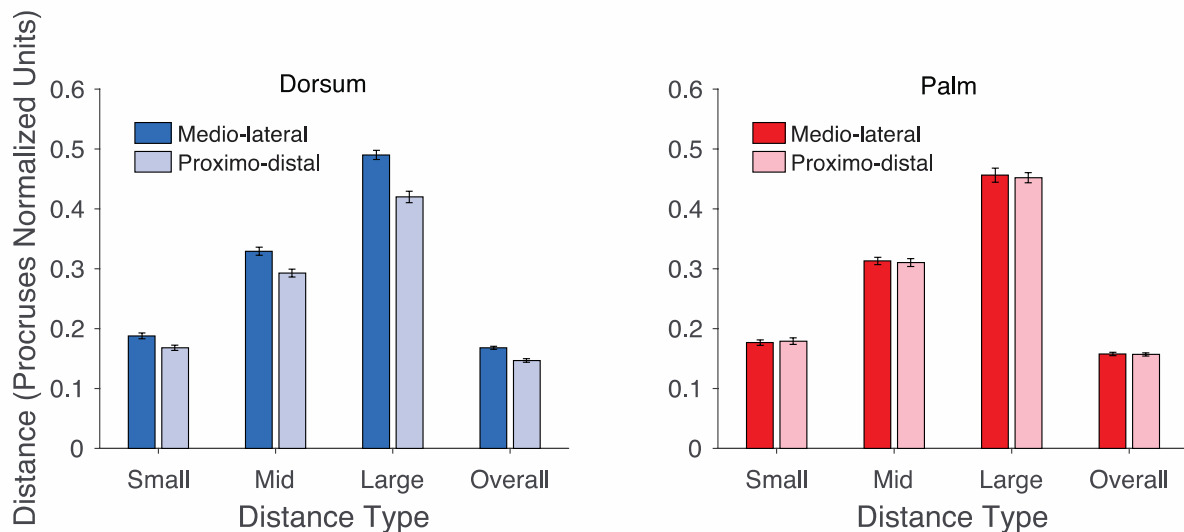

Figure 8: Mean distance in Procrustes normalized space between pairs of landmarks in the medio-lateral and proximo-distal orientations in Experiment 2 on the dorsum (left panel, blue) and palm (right panel, red). As in Experiment 1, there was clear overestimation of distances in the medio-lateral orientation on the dorsum; no such effect, however, was apparent on the palm. Error bars are one standard error of the mean.

Figure 9 shows mean Procrustes distances of maps with square grids stretched by different amounts. For the dorsum, the mean best-fitting stretch parameter was 1.185, significantly greater than both 1, $t(20) = 3.58$, $p < 0.002$, $d = 0.78$, and the mean

parameter from the actual configuration, $t(20) = 5.05$, $p < 0.0001$, $d_z = 1.10$. In contrast,

the best-fitting stretch on the palm (0.999) did not differ significantly either from 1,

$t(20) = -0.01$, *n.s.*, $d = 0.00$, nor from the mean parameter of actual maps, $t(20) = 1.13$,

n.s., $d = 0.25$. The best-fitting stretch parameter was significantly greater on the dorsum

than on the palm, both for raw parameters, $t(20) = 2.40$, $p < 0.05$, $d_z = 0.52$, and the

difference between parameters for judged and actual maps, $t(20) = 2.60$, $p < 0.02$, $d_z =$

0.57. Thus, the distortion was larger on the hairy skin of the hand dorsum than on the

glabrous skin of the palm, consistent with other results (e.g., Longo & Haggard, 2011).

As in Experiment 1, best-fitting stretch parameters for the actual configuration of

landmarks were slightly, though significantly, less than 1, both for the dorsum (*M*:

0.933), $t(20) = -10.12$, $p < 0.0001$, $d = 2.21$, and the palm (*M*: 0.949), $t(20) = -4.46$, $p <$
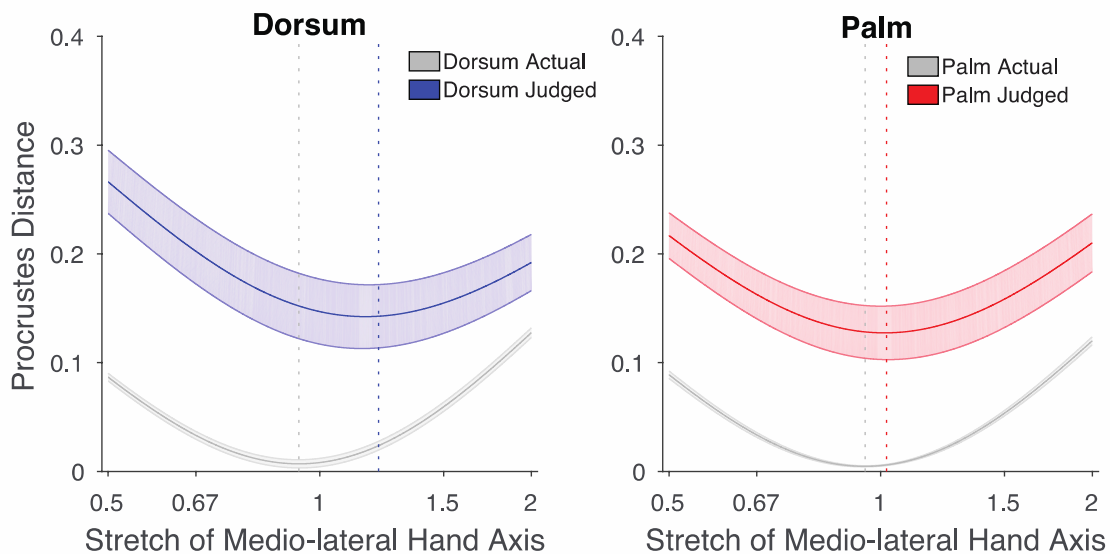
0.0005, $d = 0.97$.

Figure 9: Mean Procrustes distance as a function of stretch in Experiment 2 between perceptual maps on the dorsum (left panel, blue) and palm (right panel, red) and actual maps (grey in both panels). A stretch of 1 indicates a square grid; stretches greater than 1 indicate stretch in the medio-lateral axis, while stretches less than 1 indicate stretch in the proximo-distal axis. The shaded regions indicate one standard error of the mean. As in Experiment 1, the best-fitting stretch was greater than 1 for perceptual maps on the dorsum, indicate stretch in the medio-lateral axis. In contrast, no such deviation from a perfectly square grid was apparent on the palm.

General Discussion

We constructed perceptual maps of the internal geometry of tactile space using MDS. We showed that the two-dimensional structure of the skin can be reconstructed from the matrix of perceived distances between touches applied to pairs of locations. In Experiment 1 we showed that tactile space is stretched along the medio-lateral axis of the hand dorsum. Experiment 2 replicated this finding, and showed that no similar distortion is apparent on the glabrous skin of the palm. Our method provides a novel tool to map the mental representation of the body and to explore spatial distortions of tactile space.

Body-Scaled Information for Tactile Perception

The paper by Warren and Whang (1987) drew attention to the role of body-scaled information in the visual perception of affordances. As discussed in the introduction, numerous studies have shown that manipulations of perceived body-part size produce corresponding changes in the perception of tactile distance (e.g., Taylor-Clarke et al., 2004; de Vignemont et al., 2005; Tajadura-Jiménez et al., 2012; Miller et al., 2014). Such manipulations are analogous to the classic use of a false floor to manipulate apparent eyeheight in Warren and Whang's paper, and demonstrate the importance of body-scaled information in the sense of touch.

According to the pixel model (Longo & Haggard, 2011; Longo, 2017), the distortions we describe here result from the anisotropic geometry of RFs in somatosensory cortex (e.g., Alloway et al., 1989; Brooks et al., 1961) rather than from higher-order body representations. How then does body-scaled information affect the perception of tactile distance? One potential source of insight into this question comes from the fact that distortions of tactile distance perception are much smaller than would be predicted purely on the basis of differences in RF size and shape. In owl monkeys, for

example, the magnification levels on different skin surfaces differ by two orders of magnitude (e.g., Sur, Merzenich, & Kaas, 1980). While the differences in perceived tactile distance across skin surfaces seen in Weber's illusion parallel these differences, they are dramatically smaller in magnitude (Taylor-Clarke et al., 2004; Longo, 2017). Similarly, the long axis of RFs in somatosensory cortex is frequently 4-5 times the length of the small axis (e.g., Brooks et al., 1961), yet the magnitude of perceptual anisotropy is again only a small fraction of that (e.g., Green, 1982; Longo & Haggard, 2011; this study). Higher-level body representations may thus influence tactile perception at processing stages beyond primary somatosensory cortex to correct for homuncular distortions, a form of tactile size constancy. Linkenauger and colleagues (2015) recently suggested that such constancy might be achieved by integrating distorted homunculus signals with a representation of the body with exactly opposite distortions, what they call 'reverse distortion'. Alternatively, information about true body size may be embedded in a set of scaling parameters which result in body maps in posterior parietal cortex having more proportional representations of the skin than those in primary somatosensory cortex (Longo, 2017).

Distortions of Tactile Space are Geometrically Coherent

The pixel model (Longo & Haggard, 2011; Longo, 2017) proposes that tactile space is comprised of a two-dimensional array in which each unit is a single somatosensory RF. Where RFs differ in size on different skin surfaces, this will produce a perceptual magnification on the surface with smaller RFs. Where individual RFs are anisotropic (e.g., oval-shaped), this will produce a perceptual stretch along the shorter axis of the RF. In each case, the distortions induced can be characterized by geometrically coherent deformations (i.e., stretches) of tactile space. The current results

are consistent with this model in showing that the anisotropies previous reported for tactile distance on the hand (e.g., Green, 1982; Longo & Haggard, 2011) can be characterized as a simple stretch of tactile space along the medio-lateral hand axis (or, equivalently, as compression of the proximo-distal axis). This pattern is consistent with the predictions of the pixel model given that somatosensory RFs on the hairy skin of the limbs tend to be oval-shaped with the long-axis aligned with the proximo-distal limb axis (e.g., Brooks et al., 1961; Alloway et al., 1989).

Interestingly, the degree of geometric coherence seen in the present study in the case of tactile distance does not appear to characterize spatial anisotropy in vision. Howe and Purves (2002) compiled data from a number of studies of the visual horizontal-vertical illusion to investigate perceived size not just for perfectly vertical and horizontal lines, but across a full range of orientations. In fact, lines were perceived as longest not when exactly vertical, but when rotated approximately 20° in either direction from the vertical. Such a dual-peak pattern is inconsistent with perceived length reflecting a simple stretch of visual space, in which case the function relating orientation to perceived size should be sinusoidal. To our knowledge, no study has investigated perceived tactile distance similarly as a function of orientation. On the basis of the present results, we would predict that unlike in vision, perceived tactile distance should change smoothly as a function of orientation.

Tactile Distances in 2-D and 3-D Space

The dorsum of the hand is largely a flat, two-dimensional surface, but not perfectly. For most people, there is some degree of curvature, particularly in the medio-lateral hand axis. Resting one's hand on a flat surface, the centre of the hand is a bit higher off the surface than the sides towards the little finger or thumb. This curvature

was apparent in the present study in terms of the actual configuration of locations on participants' hands being best fit by a grid stretched slightly in the proximo-distal axis (i.e., a stretch parameter less than 1). This is because the curvature of the hand (convex on the dorsum; concave on the palm) results in points along the medio-lateral axis being slightly closer together 'as the crow flies' in their projection onto the plane of the photograph taken.

This raises the point that there are two ways in which the distance between two stimulated points on the skin might be conceived. First, distance could be thought of in terms of distance along the surface of the skin (i.e., the distance that an ant walking on the skin between the two points would traverse). Second, distance could be thought of in terms of the 3-D Euclidean distance of the shortest path between the stimulated points (i.e., going *through* the flesh of the hand). Participants in the present study were given no specific instructions about how to conceive of distance, and are unlikely to have thought about these two potential meanings. We have previously interpreted the fact that the magnitude of anisotropy is different on the two sides of the hand as evidence that tactile distances are interpreted in 2-D skin space (Longo, 2015). The present results are consistent with this interpretation, since the distortion on the two sides of the hand is different. If it were the representation of the hand as a volumetric object that were stretched, this distortion should be apparent on both sides of the hand. Instead, the distortion is only apparent on the dorsal hand surface, suggesting that it is a 2-D representation of each skin surface which is distorted, rather than a 3-D representation of the hand as a volumetric object.

MDS as a Tool for Mapping Perceptual Spaces

Several previous studies have attempted to construct perceptual maps of the body surface. Trojan and colleagues (2006, 2009) applied nociceptive stimuli to the forearm with a CO_2 laser and asked participants to localize each stimuli in external space using a stylus. They reported patterns of mislocalisation along the proximo-distal axis which were consistent within individuals, but differed idiosyncratically between people. Longo and Haggard (2010, 2012) developed a procedure for mapping representations of the hand underlying position sense. Participants placed their hand flat on a table underneath an occluding board and used a long baton to judge the perceived location of the tip and knuckle of each finger. By comparing the relative location of judgments of each landmark, they constructed perceptual maps of hand structure which they then compared to actual hand form. A highly consistent pattern of distortions was apparent across participants, including overestimation of hand width, and underestimation of finger length. Longo, Mancini, and Haggard (2015) conducted a similar study, but asked participants to judge the location of tactile stimuli applied to the hand dorsum, finding overestimation of distances in the medio-lateral hand axis, compared to the proximo-distal axis. It is interesting to note that this pattern of distortions is quite similar to that described in the present study for judgments of tactile distance. This is consistent with the possibility that a similarly distorted body model may underlie body position sense and tactile distance perception (cf. Longo et al., 2010), although a recent study from our lab showed that the magnitude of distortions in the two maps was not correlated across participants (Longo & Morcom, 2016).

Other studies have constructed perceptual maps in a body-centered, rather than an external, frame of reference. Rapp, Hendel, and Medina (2002), for example, asked participants to localize tactile stimuli by pointing to the perceived location of touch on their hand. They found that two individuals with damage to the left cerebral

hemisphere showed systematic patterns of mislocalisation, which preserved the relative topography of locations, but were translated and compressed compared to healthy controls. Mancini and colleagues (Mancini, Longo, Iannetti, & Haggard, 2011) asked participants to judge the perceived location of stimuli by clicking the mouse cursor on the corresponding location on a silhouette image of their hand. They found a highly-consistent pattern of distal biases on the hairy skin of the hand dorsum, which did not appear at all on the glabrous skin of the palm. The present approach differs from all these previous methods in that it does not involve any form of localization judgment. MDS allows perceptual maps to be constructed from the pattern of judgments of distance between pairs of stimuli, rather than the perceived location of individual stimuli.

The present use of MDS also differs from most previous uses in the psychological literature, in which the distance in psychological space between two stimuli or concepts is taken metaphorically to reflect perceived similarity or degree of generalization (Shepard, 1980). Our use is, in this sense, much less metaphorical since distance in the MDS solution is related directly to perceived distance, rather than to some more abstract relation between stimuli (see Aznar-Casanova et al., 2006, for a somewhat similar approach to visual stimuli). It is exactly this which allowed us to quantify spatial distortions in perceptual maps, since we have access to the ground truth of the true spatial layout, which does not exist when using MDS to investigate, to take just one example, the mental representation of musical instruments (Kendall & Certerette, 1991). MDS may be a useful tool for mapping the geometric structure of other types of perceptual spaces as well.

References

Alloway, K. D., Rosenthal, P., & Burton, H. (1989). Quantitative measurement of receptive field changes during antagonism of GABAergic transmission in primary somatosensory cortex of cats. *Experimental Brain Research, 78,* 514-532.

Anema, H. A., Wolswijk, V. W., Ruis, C., & Dijkerman, H. C. (2008). Grasping Weber's illusion: The effect of receptor density differences on grasping and matching. *Cognitive Neuropsychology, 25*, 951-967.

Aznar-Casanova, J. A., Matsushima, E. H., Ribeiro-Filho, N. P., & Da Silva, J. A. (2006). One-dimensional and multi-dimensional studies of the exocentric distance estimates in frontoparallel plane, virtual space, and outdoor open field. *Spanish Journal of Psychology, 9*, 273-284.

Banks, M. S. (1988). Visual recalibration and the development of contrast and optical flow perception. In A. Yonas (Ed.), *The Minnesota symposia on child psychology Vol. 20* (pp. 145-196). Hillsdale, NJ: Erlbaum.

Berryman, L. J., Yau, J. M., & Hsiao, S. S. (2006). Representation of object size in the somatosensory system. *Journal of Neurophysiology, 96,* 27-39.

Blough, D. S. (1982). Pigeon perception of letters of the alphabet. *Science, 218*, 397-398.

Bookstein, F. L. (1991). *Morphometric tools for landmark data: Geometry and biology*. Cambridge: Cambridge University Press.

Bosten, J. M., Robinson, J. D., Jordan, G., & Mollon, J. D. (2005). Multidimensional scaling reveals a color dimension unique to 'color-deficient' observers. *Current Biology, 15*, R950-R952.

Brooks, V. B., Rudomin, P., & Slayman, C. L. (1961). Peripheral receptive fields of neurons in the cat's cerebral cortex. *Journal of Neurophysiology, 24,* 302-325.

Bruno, N., & Bertamini, M. (2010). Haptic perception after a change in hand size.

Neuropsychologia, 48, 1853-1856.

Byatt, G., & Rhodes, G. (2004). Identification of own-race and other-race faces:

Implications for the representation of race in face space. *Psychonomic Bulletin and Review, 11*, 735-741.

Canzoneri, E., Ubaldi, S., Rastelli, V., Finisguerra, A., Bassolino, M., & Serino, A. (2013).

Tool-use reshapes the boundaries of body and peripersonal space

representations. *Experimental Brain Research, 228*, 25-42.

Carrie, S., Scannell, J. W., & Dawes, P. J. D. (1999). The smell map: Is there a commonality

of odour perception? *Clinical Otolaryngology, 24*, 184-189.

Chang, E. F., Rieger, J. W., Johnson, K., Berger, M. S., Barbaro, N. M., & Knight, R. T. (2010).

Categorical speech representation in human superior temporal gyrus. *Nature Neuroscience, 13*, 1428-1432.

Cholewiak, R. W. (1999). The perception of tactile distance: Influences of body site,

space, and time. *Perception, 28,* 851-875.

Clark, W. C., Carroll, J. D., Yang, J. C., & Janal, M. N. (1986). Multidimensional scaling

reveals two dimensions of thermal pain. *Journal of Experimental Psychology: Human Perception and Performance, 12*, 103-107.

Clark, W. C., Ferrer-Brechner, T., Janal, M. N., Carroll, J. D., & Yang, J. C. (1989). The

dimensions of pain: A multidimensional scaling comparison of cancer patients

and healthy volunteers. *Pain, 37*, 23-32.

Clifton, R. K., Gwiazda, J., Bauer, J. A., Clarkson, M. G., & Held, R. M. (1988). Growth in

head size during infancy: Implications for sound localization. *Developmental Psychology, 24*, 477-483.

Cody, F. W. J., Gaarside, R. A. D., Lloyd, D., & Poliakoff, E. (2008). Tactile spatial acuity

varies with site and axis in the human upper limb. *Neuroscience Letters, 433,* 103-108.

Cox, T. F., & Cox, M. A. A. (2001). *Multidimensional scaling, 2nd Ed.* London: Chapman and Hall.

Cutzu, F., & Edelman, S. (1996). Faithful representation of similarities among three-dimensional shapes in human vision. *Proceedings of the National Academy of Sciences, USA, 93*, 12046-12050.

de Vignemont, F., Ehrsson, H. H., & Haggard, P. (2005). Bodily illusions modulate tactile perception. *Current Biology, 15,* 1286-1290.

DiCarlo, J. J., & Johnson, K. O. (2002). Receptive field structure in cortical area 3b of the alert monkey. *Behavioural Brain Research, 135,* 167-178.

DiCarlo, J. J., Johnson, K. O., & Hsiao, S. S. (1998). Structure of receptive fields in area 3b of primary somatosensory cortex in the alert monkey. *Journal of Neuroscience, 18,* 2626-2645.

Everitt, B. S., & Rabe-Hesketh, S. (1997). *The analysis of proximity data*. London: Arnold.

Feldman Barrett, L., & Fossum, T. (2001). Mental representation of affect knowledge. *Cognition and Emotion, 15*, 333-363.

Friston, K. J., Frith, C. D., Fletcher, P., Liddle, P. F., & Frackowiak, R. S. J. (1996). Functional topography: Multidimensional scaling and functional connectivity in the brain. *Cerebral Cortex, 6*, 156-164.

Fuentes, C. T., Longo, M. R., & Haggard, P. (2013). Body image distortions in healthy adults. *Acta Psychologica, 144*, 344-351.

Fuentes, C. T., Pazzaglia, M., Longo, M. R., Scivoletto, G., & Haggard, P. (2013). Body image distortions following spinal cord injury. *Journal of Neurology, Neurosurgery, and Psychiatry, 84*, 201-207.

Gärdenfors, P. (2000). *Conceptual spaces: The geometry of thought*. Cambridge, MA: MIT Press.

Goodall, C.R., 1991. Procrustes methods in the statistical analysis of shape. *Journal of the Royal Statistical Society, 53*, 285–339.

Green, B. E. (1982). The perception of distance and location for dual tactile pressures. *Perception and Psychophysics, 31,* 315-323.

Griffiths, T. L., & Kalish, M. L. (2002). A multidimensional scaling approach to mental multiplication. *Memory and Cognition, 30*, 97-106.

Hollins, M., Bensmaïa, S., Karlof, K., & Young, F. (2000). Individual differences in perceptual space for tactile textures: Evidence from multidimensional scaling. *Perception and Psychophysics, 62*, 1534-1544.

Howe, C. Q., & Purves, D. (2002). Range image statistics can explain the anomalous perception of length. *Proceedings of the National Academy of Sciences, USA, 99*, 13184-13188.

Johnson, E. J., & Tversky, A. (1984). Representations of perceptions of risks. *Journal of Experimental Psychology: General, 113*, 55-70.

Kendall, R. A., & Carterette, E. C. (1991). Perceptual scaling of simultaneous wind instrument timbres. *Music Perception, 8*, 369-404.

Kriegeskorte, N., Mur, M., Ruff, D. A., Kiani, R., Bodurka, J., Esteky, H., Tanaka, K., & Bandettini, P. A. (2008). Matching categorical object representations in inferior temporal cortex of man and monkey. *Neuron, 60*, 1126-1141.

Kring, A. M., Feldman Barrett, L., & Gard, D. E. (2003). On the broad applicability of the affective circumplex: Representations of affective knowledge among schizophrenia patients. *Psychological Science, 14*, 207-214.

Krumhansl, C. L., & Kessler, E. J. (1982). Tracing the dynamic changes in perceived tonal

organization in a spatial representation of musical keys. *Psychological Review, 89*, 334-368.

Le Cornu Knight, F., Longo, M. R., & Bremner, A. J. (2014). Categorical perception of tactile distance. *Cognition, 131*, 254-262.

Linkenauger, S. A., Wong, H. Y., Geuss, M., Stefanucci, J. K., McCulloch, K. C., Bülthoff, H. H., Mohler, B. J., & Proffitt, D. R. (2015). The perceptual homunculus: The perception of the relative proportions of the human body. *Journal of Experimental Psychology: General, 144*, 103-113.

Longo, M. R. (2015). Implicit and explicit body representations. *European Psychologist, 20*, 6-15.

Longo, M. R. (2017). Distorted body representations in healthy cognition. *Quarterly Journal of Experimental Psychology, 70*, 378-388.

Longo, M. R., Azañón, E., & Haggard, P. (2010). More than skin deep: Body representation beyond primary somatosensory cortex. *Neuropsychologia, 48,* 655-668.

Longo, M. R., Ghosh, A., & Yahya, T. (2015). Bilateral symmetry of distortions of tactile size perception. *Perception, 44*, 1251-1262.

Longo, M. R., & Haggard, P. (2010). An implicit body representation underlying human position sense. *Proceedings of the National Academy of Sciences, USA, 107,* 11727-11732.

Longo, M. R., & Haggard, P. (2011). Weber's illusion and body shape: Anisotropy of tactile size perception on the hand. *Journal of Experimental Psychology: Human Perception and Performance, 37*, 720-726.

Longo, M. R., & Haggard, P. (2012). A 2.5-D representation of the human hand. *Journal of Experimental Psychology: Human Perception and Performance, 38*, 9-13.

Longo, M. R., & Morcom, R. (2016). No correlation between distorted body representations underlying tactile distance perception and position sense. *Frontiers in Human Neuroscience, 10*, 593.

Longo, M. R., & Sadibolova, R. (2013). Seeing the body distorts tactile size perception. *Cognition, 126*, 475-481.

Longo, M. R., Mancini, F., & Haggard, P. (2015). Implicit body representations and tactile spatial remapping. *Acta Psychologica, 160*, 77-87.

Mancini, F., Longo, M. R., Iannetti, G. D., & Haggard, P. (2011). A supramodal representation of the body surface. *Neuropsychologia, 49*, 1194-1201.

Miller, L. E., Longo, M. R., & Saygin, A. P. (2014). Tool morphology constrains the effects of tool use on body representations. *Journal of Experimental Psychology: Human Perception and Performance, 40*, 2143-2153.

Miller, L. E., Longo, M. R., & Saygin, A. P. (2016). Mental body representations retain homuncular shape distortions: Evidence from Weber's illusion. *Consciousness and Cognition, 40*, 17-25.

Miller, L. E., Longo, M. R., & Saygin, A. P. (2017). Visual illusion of tool use recalibrates tactile perception. *Cognition, 162*, 32-40.

Nosofsky, R. M. (1986). Attention, similarity, and the identification-categorization relationship. *Journal of Experimental Psychology: General, 115*, 39-57.

Oldfield, R. C. (1971). The assessment and analysis of handedness: The Edinburgh inventory. *Neuropsychologia, 9,* 97-113.

Penfield, W., & Boldrey, E. (1937). Somatic motor and sensory representation in the cerebral cortex of man as studied by electrical stimulation. *Brain, 60,* 389-443.

Powell, T. P. S., & Mountcastle, V. B. (1959). Some aspects of the functional organization

of the cortex of the postcentral gyrus of the monkey: A correlation of findings obtained in a single unit analysis with cytoarchitecture. *Bulletin of the Johns Hopkins Hospital, 105*, 133-162.

Rapp, B., Hendel, S. K., & Medina, J. (2002). Remodeling of somatosensory hand representations following cerebral lesions in humans. *NeuroReport, 13*, 207-211.

Rhodes, G. (2013). Looking at faces: First-order and second-order features as determinants of facial appearance. *Perception, 42*, 1179-1199.

Rholf, F. J., & Slice, D. E. (1990). Extensions of the Procrustes methods for the optimal superimposition of landmarks. *Systematic Zoology, 39*, 40-59.

Shepard, R. N. (1980). Multidimensional scaling, tree-fitting, and clustering. *Science, 210*, 390-398.

Shepard, R. N. (1982). Geometrical approximations to the structure of musical pitch. *Psychological Review, 89*, 305-333.

Shepard, R. N. (1987). Toward a universal law of generalization for psychological science. *Science, 237*, 1317-1323.

Shepard, R. N., & Cooper, L. A. (1992). Representation of colors in the blind, color-blind, and normally sighted. *Psychological Science, 3*, 97-104.

Sur, M., Merzenich, M. M., & Kaas, J. H. (1980). Magnification, receptive-field area, and "hypercolumn" size in areas 3b and 1 of somatosensory cortex in owl monkeys. *Journal of Neurophysiology, 44*, 295-311.

Tajadura-Jiménez, A., Väljamäe, A., Toshima, I., Kimura, T., Tsakiris, M., & Kitagawa, N. (2012). Action sounds recalibrate perceived tactile distance. *Current Biology, 22*, R516-R517.

Tajadura-Jiménez, A., Tsakiris, M., Marquardt, T., & Bianchi-Berthouze, N. (2015). Action

sounds update the mental representation of arm dimension: Contributions of

kinaesthesia and agency. *Frontiers in Psychology, 6*, 689.

Taylor-Clarke, M., Jacobsen, P., & Haggard, P. (2004). Keeping the world a constant size:

Object constancy in human touch. *Nature Neuroscience, 7*, 219-220.

Thompson, D. W. (1917). *On growth and form*. Cambridge: Cambridge University Press.

Trojan, J., Kleinböhl, D., Stolle, A. M., Andersen, O. K., Hölzl, R., & Arendt-Nielsen, L.

(2006). Psychophysical 'perceptual maps' of heat and pain sensations by direct

localization of CO_2 laser stimuli on the skin. *Brain Research, 1120*, 106-113.

Trojan, J., Kleinböhl, D., Stolle, A. M., Andersen, O. K., Hölzl, R., & Arendt-Nielsen, L.

(2009). Independent psychophysical measurement of experimental modulations

in the somatotopy of cutaneous heat-pain stimuli. *Somatosensory and Motor

Research, 26*, 11-17.

Warren, W. H., & Whang, S. (1987). Visual guidance of walking through apertures: Body-

scaled information for affordances. *Journal of Experimental Psychology: Human

Perception and Performance, 13,* 371-383.

Weber, E. H. (1996). *De subtilitate tactus* (H. E. Ross, Trans.). In H. E. Ross & D. J. Murray

(Eds.), *E. H. Weber on the tactile senses, 2nd ed* (pp. 21-128). London: Academic

Press. (Original work published 1834)

Wolff, P., & Song, G. (2003). Models of causation and the semantics of causal verbs.

Cognitive Psychology, 47, 276-332.

Young, M. P., & Yamane, S. (1992). Sparse population coding of faces in the

inferotemporal cortex. *Science, 256*, 1327-1331.

Acknowledgments